PLANETARY EFFECTS ON MAGNETIC ACTIVITY

by

GERALD ATKINSON

B.A.Sc., University of British Columbia, 1960

A THESIS SUBMITTED IN PARTIAL FULFILMENT OF

THE REQUIREMENTS FOR THE DEGREE OF

MASTER OF SCIENCE

in the Department

of

GEOPHYSICS

We accept this thesis as conforming to the

required standard

THE UNIVERSITY OF BRITISH COLUMBIA

August, 1964.

In presenting this thesis in partial fulfilment of the requirements for an advanced degree at the University of British Columbia, I agree that the Library shall make it freely available for reference and study. I further agree that permission for extensive copying of this thesis for scholarly purposes may be granted by the Head of my Department or by his representatives. It is understood that copying or publication of this thesis for financial gain shall not be allowed without my written permission.

Department of Geophysics

The University of British Columbia,
Vancouver 8, Canada

Date 5 September, 1964

ABSTRACT

Statistical evidence indicates that the positions of the moon, Mercury, and Venus affect magnetic activity frequency observed at the earth, and the position of the earth affects the frequency of blue clearings on Mars. This study shows that these effects may be explained as a result of the action of shock and bow waves formed by these bodies in the supersonically streaming interplanetary plasma. The attenuation of large kinetic energy variations in the streaming plasma behind such bodies is shown to be equal to the square of the ratio of the Mach number upstream to the Mach number downstream. For typical solar induced activity, this implies an attenuation coefficient of approximately 1/2 - 1/3. It is also shown that an activity increase is expected in the bow wave. The observational data fits a model with bow waves of Mach numbers 2.5 and 15 corresponding to the two bow waves predicted by the theory. The moon's effect varies from that of the planets in a manner that can be explained by its closeness to the magnetosphere.

ACKNOWLEDGMENT

I am deeply indebted to Dr. T. Watanabe both for his patient supervision, and for his many hours of discussion of the ideas expressed in this thesis. I would also like to thank Professor J. A. Jacobs for his encouragement during the preparation of this work, and for his guidance in its final formulation.

TABLE OF CONTENTS

TABLES

APPENDIX

FIGURES

I. INTRODUCTION

Bigg (1963 a, b) has presented statistical evidence for lunar and planetary influences on magnetic activity as observed at the earth's surface. There are peaks of activity frequency when the planet is at large distances from the sun-earth line, indicating an effect over a region of much greater size than the physical dimensions of the body. This thesis attempts to explain this phenomenon as the result of the bow shock wave formed by an object in a supersonic stream. The object is a planet or the moon, and the stream is the solar wind and any particle clouds or streams which are emitted by the sun. The flow is supersonic to magnetohydrodynamic waves within it.

The symbolism used throughout will be conventional, and is listed in the Appendix. It will not be further explained within the text except where the author feels that it is unclear or unconventional.

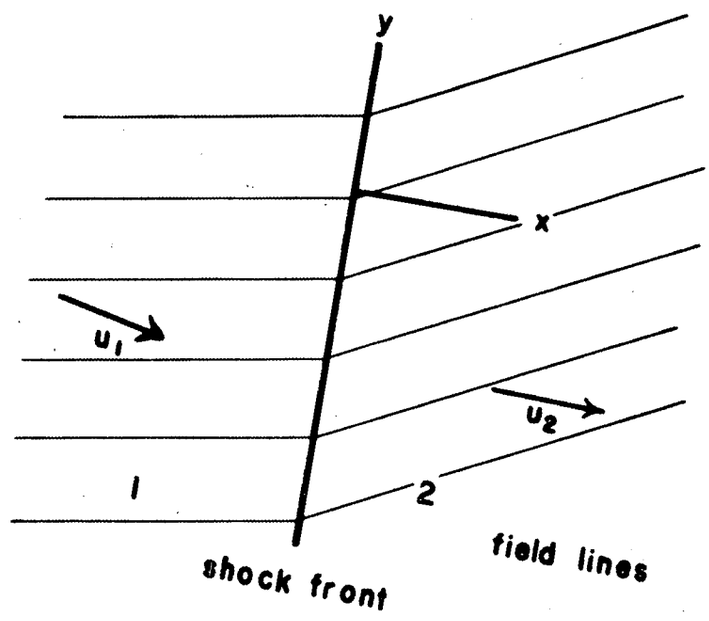

Figure 1. Geometry for the shock equations.

II. THE BOW WAVE

a. Hydromagnetic shocks

The basic relations for hydromagnetic shocks are the De Hoffmann-Teller equations. An excellent derivation of them is given by Bershader (1959, pp. 18-20). If a rectangular coordinate system is chosen such that the x axis is normal to the plane of the shock front and the y and z axes lie within the plane, the equations have the following form:

(1) Conservation of mass

$$\left[\rho u_x\right]_1^2 = 0$$

(2) Conservation of field lines

a. $$\left[B_x\right]_1^2 = 0$$

b. $$\left[u_x B_y\right]_1^2 = \left[u_y B_x\right]_1^2$$

c. $$\left[u_x B_z\right]_1^2 = \left[B_x u_z\right]_1^2$$

(3) Conservation of momentum

a. $$\left[p + \rho u_x^2 + \frac{B_z^2 + B_y^2}{2\mu_0}\right]_1^2 = 0$$

b. $$\left[\rho u_x u_y - \frac{B_x B_y}{\mu_0}\right]_1^2 = 0$$

c. $$\left[\rho u_x u_z - \frac{B_x B_z}{\mu_0}\right]_1^2 = 0$$

(4) Conservation of energy

$$\left[\frac{1}{2}u^2 + \frac{\gamma}{\gamma-1}\frac{p}{\rho} + \frac{B^2 u_x - (\vec{B}\cdot\vec{u})B_x}{\mu_0 \rho u_x}\right]_1^2 = 0$$

$\left[\ \right]_1^2$ denotes the value of the expression in the brackets behind the shock minus its value in front of the shock.

These equations are too complicated to use in this form in an analysis of the bow shock wave in a three dimensional situation. Kellogg (1962), Spreiter and Jones (1963) and Obayashi (1964) use the Rankine-Hugoniot relations for an ordinary gas, taking values of $\gamma = \frac{c_p}{c_v}$ from 5/3 to 2 depending on the number of dimensions involved in the compression.

The assumption in this approach is that $B_x = 0$, which simplifies the De Hoffmann-Teller relations to the following form:

(5) Conservation of mass

$$\left[\rho u_x\right]_1^2 = 0$$

(6) Conservation of field lines

$$\left[u_x(\vec{B}_y + \vec{B}_z)\right]_1^2 = \left[u_x \vec{B}\right]_1^2 = 0$$

(7) Conservation of momentum

a. $$\left[p + \rho u_x^2 + \frac{B^2}{2\mu_0}\right]_1^2 = 0$$

b. $$\left[\rho u_x (\vec{u_y} + \vec{u_z})\right]_1^2 = 0$$

or $$\left[\vec{u_t}\right]_1^2 = 0 \qquad \text{(using 5)}$$

where u_t denotes the component of $\vec{u}$ tangential to the shock plane.

(8) Conservation of energy

$$\left[\frac{1}{2}u^2 + \frac{\gamma}{\gamma - 1}\frac{p}{\rho} + \frac{B^2}{\mu_0 \rho}\right]_1^2 = 0$$

As B is assumed to be everywhere perpendicular to the shock front, it exerts only a pressure across the front, and can therefore be treated as a gas ($\gamma = 2$) of pressure $p_{mag} = \frac{B^2}{2\mu_0}$. The equations then become:

(9) Conservation of mass

$$\left[\rho u_x\right]_1^2 = 0$$

(10) Conservation of field lines

$$\left[u_x \vec{B}\right]_1^2 = 0$$

(11) Conservation of momentum

a. $$\left[p + p_{mag} + \rho u_x^2\right]_1^2 = \left[P + \rho u_x^2\right]_1^2 = 0$$

b. $$\left[u_t\right]_1^2 = 0$$

(12) Conservation of energy

$$\left[\frac{1}{2}u^2 + \frac{\gamma}{\gamma-1}\frac{p}{\rho} + \frac{\gamma_{mag}}{\gamma_{mag}-1}\frac{p_{mag}}{\rho}\right]_1^2$$

$$= \left[\frac{1}{2}u^2 + \frac{\gamma^*}{\gamma^*-1}\frac{p}{\rho}\right]_1^2 = 0$$

where $$P = p + p_{mag}$$

and $$\gamma \leq \gamma^* \leq \gamma_{mag} = 2$$

If $p_{mag} >> p$, $\gamma^* = 2$, and if $p >> p_{mag}$, $\gamma^* = \gamma$.

In this form, equations 9, 11, 12 are identical with the Rankine-Hugoniot equations. Equation 10 is an extra one which merely serves to specify the magnetic field.

The largest error created by the assumption that $B_x = 0$ lies in the neglect of magnetic tension terms that should arise from field lines crossing the interface. If the field in the incoming plasma is perpendicular to the velocity, and is incident on a spherical shock front, $\vec{B}$ is parallel to the front only on a great circle perpendicular to $\vec{B}$. The approximation may thus be quite good on a strip near the great circle, but farther back towards the axis of this circle magnetic tension terms may become important.

It must further be noted in applying this theory to the earth that inside the shocked region $\frac{1}{2}\rho u_1^2 \sim \frac{B^2}{2\mu_0}$ (from satellite measurements). Thus the hydrodynamic forces do not predominate over the field forces as is the case in the incident stream.

b. Hydromagnetic waves

In dealing with the bow wave at distances large compared to the dimensions of the body, a wave approach is easier than an extension of the discussion of one dimensional shocks. At frequencies near and below the ion cyclotron frequency (ω_i), there are three modes by which electromagnetic waves can propagate. This thesis is concerned mainly with low frequencies and will henceforth refer to them by their hydromagnetic names. The nomenclature of

Denisse and Delcroix (1963) will be used. The discussion will be limited for the present to the case $\omega \ll \omega_i$, and to dense plasmas — plasmas in which the hydromagnetic velocities are much less than the speed of light. Under such conditions, all three modes are non-dispersive, and, to the first order, electrically neutral. The ions and electrons move together.

The oblique Alfven mode has a phase velocity:

(13) $$v_p^2 = V_A^2 \cos^2 \Theta$$

where Θ is the angle between the plane wave propagation vector ($\vec{k}$) and the steady magnetic field ($\vec{B}_o$). The particle displacements and the perturbing magnetic field are perpendicular to $\vec{B}_o$ and $\vec{k}$, so that there is no coupling with the other two modes which are confined to the plane defined by $\vec{B}_o$ and $\vec{k}$. The group velocity is given by $v_g^2 = V_A^2$, and is parallel to $\vec{B}_o$, indicating that energy transfer can take place only along the field lines in the oblique Alfven mode.

The accelerated and retarded magnetoacoustic modes have phase velocities given by:

(14) $$v_p^2 = \frac{V_A^2 + V_s^2 \pm \sqrt{V_A^4 + V_s^4 - 2V_A^2 V_s^2 \cos 2\Theta}}{2}$$

the + and - signs indicating accelerated and retarded modes

respectively. $V_S = \sqrt{\frac{\gamma p}{\rho}}$ is the speed of "sound" in the plasma i.e. the speed at which a compression wave will propagate through an unmagnetized plasma. The particle velocity component ratios are given by:

$$(15) \quad \frac{V_y}{V_z} = \frac{1}{\tan \Theta} \left(\frac{V_S^2}{V_P^2} - 1 \right)$$

where the coordinate axes are defined such that x is normal to $\vec{B}_o$ and $\vec{k}$, and z is parallel to $\vec{k}$. If V_A and V_S are of the same order of magnitude, the motions of the accelerated and retarded mode particles are not orthogonal, and there is coupling between the two modes. Polar velocity diagrams are shown for $V_A > V_S$ and $V_S > V_A$ in figure 2.

For the two extreme cases: $V_S >> V_A$ and $V_A >> V_S$, the coupling becomes small. If $V_A >> V_S$, the accelerated mode has a phase velocity $v_p \simeq V_A$, and the particle motion is perpendicular to $\vec{B}_o$. This mode is a combination of an Alfven wave along the field and a compressional wave across the field. The slow mode has a phase velocity $v_p = V_S \cos \Theta$, and the particle motion and energy transfer are parallel to $\vec{B}_o$, the group velocity being V_S. Conversely if $V_S >> V_A$, the fast mode has a phase velocity $v_p \simeq V_S$. The particle motion is parallel to $\vec{k}$. It is a combination of a

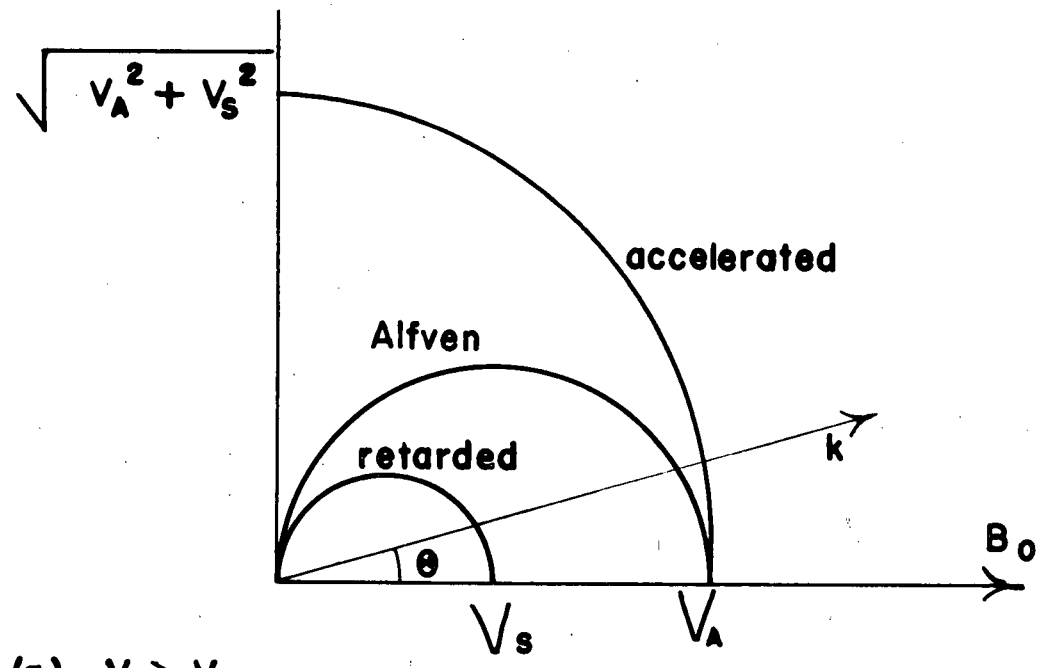

(a) $V_A > V_S$

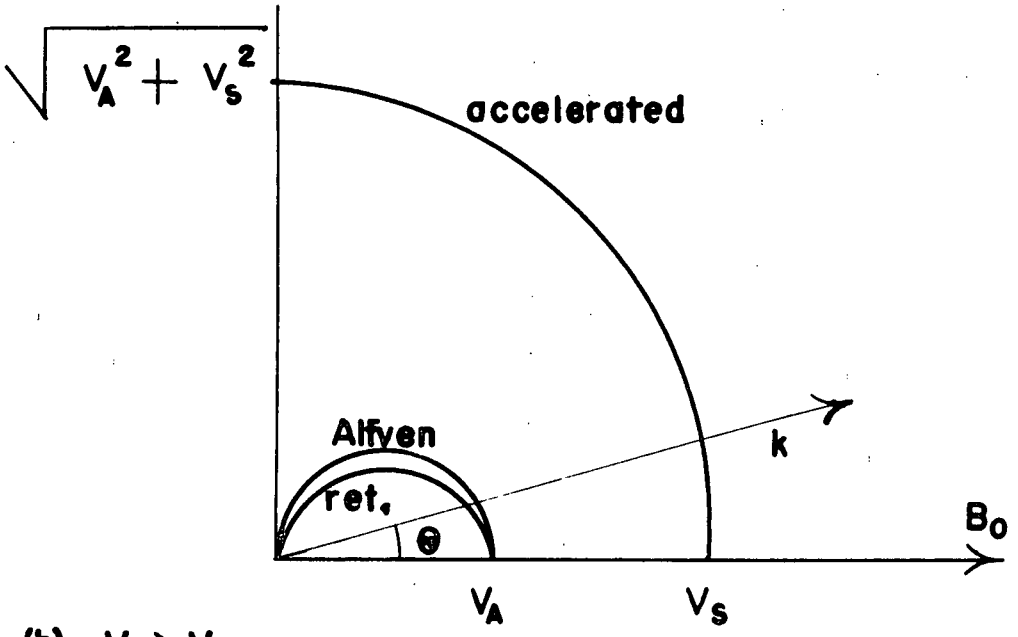

(b) $V_S > V_A$

Figure 2. Polar velocity diagrams for magnetohydrodynamic waves.

sound wave along the field line and a compressional wave perpendicular to the field. The slow mode has a phase velocity $v_p = V_A \cos \Theta$. It is very little different from an oblique Alfven wave, and represents energy transfer along the field lines. In either of these extreme cases from any given stationary source, there should be almost spherical radiation fronts in the accelerated magnetoacoustic mode, and radiation along the field lines in the retarded magnetoacoustic and Alfven modes.

Applying this to the bow wave produced in steady supersonic flow, the accelerated mode should produce an almost circular cone, and the slow mode and the Alfven mode should produce two-dimensional V's. The V will not be symmetric about the flow direction except in the case when the interplanetary field is perpendicular to the streaming velocity. It will become more symmetric with increasing Mach number.

c. Hydrodynamic blunt body problem

There have been a number of attempts to calculate the flow near a sphere submerged in a supersonic stream: Lin and Rubinov (1948); Dugundji (1948); Hida (1953); Van Dyke and Milton (1958); Van Dyke, Milton and Gordon (1959);

Inouye, Mamenu and Lomax (1962). The last three obtained results by numerical analysis, and the first three obtained analytical solutions. The approach is generally to assume Rankine-Hugoniot flow through the shock, and arbitrary flow conditions behind it. Thus for example, Hida assumes incompressible irrotational flow whereas Van Dyke et al assume compressible irrotational flow. The results are valid only in a region in front of the sphere because of the type of approximation made. Experimental observation indicates that a pattern similar to that in figure 3 is formed.

In three dimensional supersonic flow, small amplitude disturbances propagate along Mach cones. If a body is axially symmetric these can be treated as Mach lines similar to the two dimensional case. These lines are shown in figure 3. It can be seen that the rarefaction tends to catch up with the front shock and wait for the rear shock, showing that such a disturbance will attenuate more rapidly than geometry and viscosity indicate. This is referred to as the rarefaction "eating into the shock". However, despite this effect, shocks are often observed at great distances from a source compared to the source size, e.g. sonic booms from aircraft (25 miles, H.A. Wilson, Jr., 1962) and bow waves from small boats. For aircraft sonic booms, $\Delta\rho \propto \frac{1}{r^{\frac{1}{4}}}$ (H.A. Wilson, Jr.,

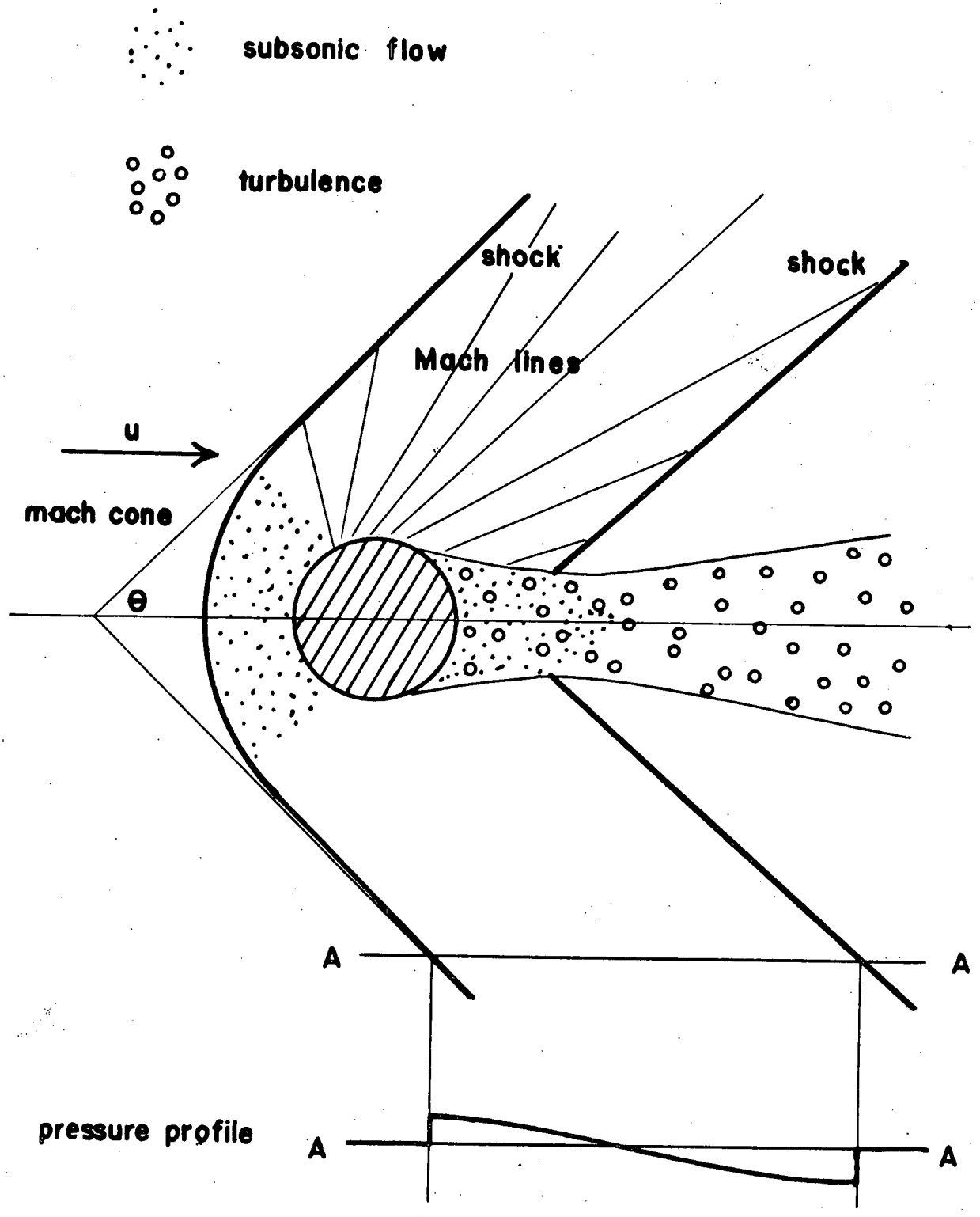

Figure 3. Supersonic flow past a sphere.

1962). This implies that the energy $\propto r^{-1.5}$.

The shock is asymptotic to a Mach cone with angle arc sin $\frac{1}{M_1}$ where M_1 is the Mach number of the incident stream. It approaches this cone as it degenerates into an ordinary small amplitude wave. The basic wavelength of the disturbance will be somewhat larger than the body size.

If the flow is quasi-steady (variations of much greater length than the body size), the principal disturbance produced should be the bow wave. Figure 4b shows the type of pattern that would be produced by constant speed sinusoidally, varying Mach number flow (which implies density fluctuations). This bow wave varies both in strength and direction. In an irregularly varying stream, a receiver at A would observe a great variety of frequencies and amplitudes.

d. Difference between hydromagnetic and hydrodynamic bow waves at large distances from the source.

Perhaps the greatest modification of the hydrodynamic picture arises from the existence of three modes of propagation in a plasma. The accelerated magnetoacoustic mode will form a Mach cone, and the oblique

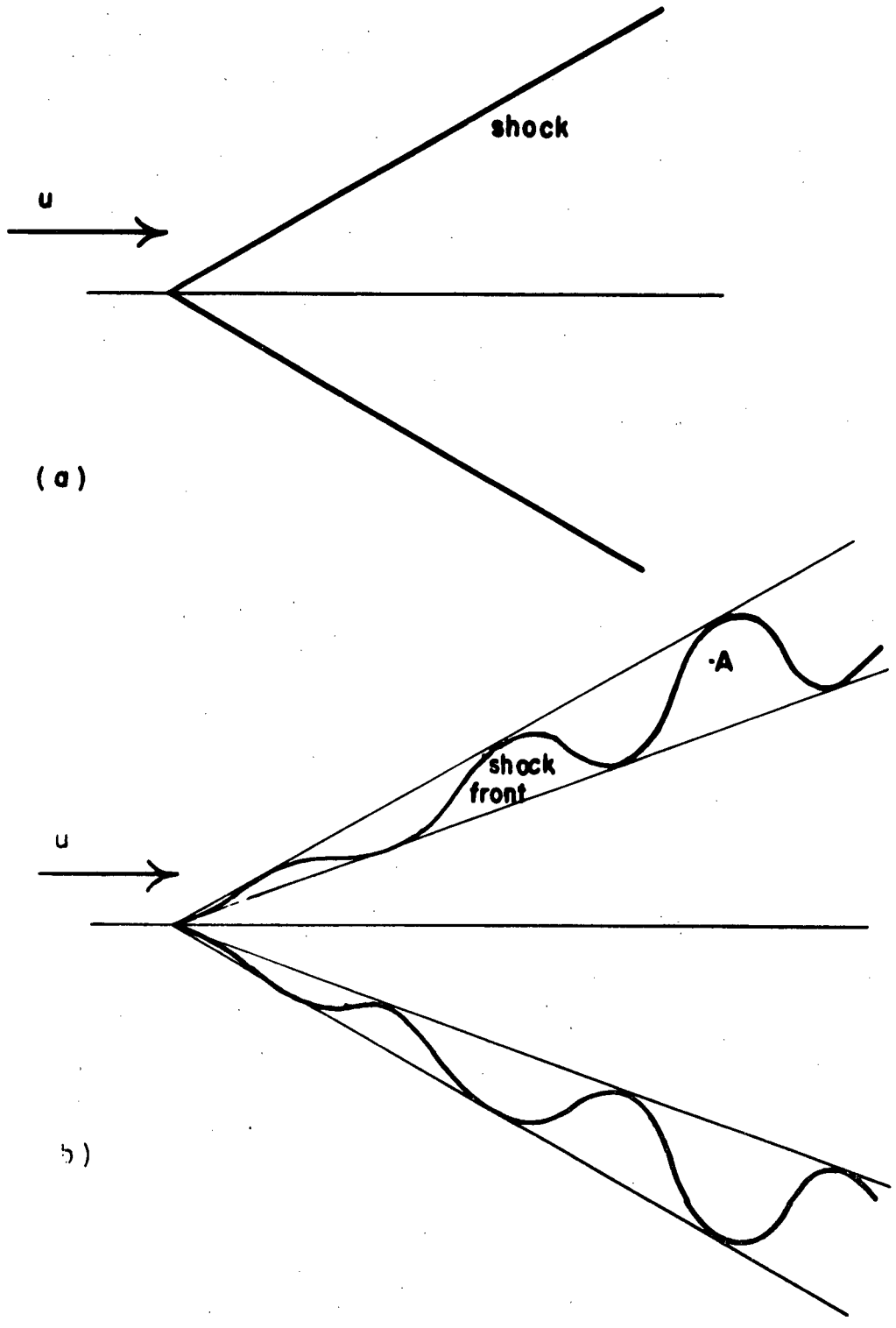

Figure 4. The bow wave. (a) steady state flow;
(b) sinusoidal Mach number - slowly varying.

Alfven and slow magnetoacoustic modes Mach V's as their group velocities are parallel to the magnetic field. The Alfven mode has the same group velocity as one of the other two, and consequently only one cone and one V will be in evidence. Over a time average of the type used by Bigg (1963 a, b), the field may be expected to take up many different orientations, and all modes of propagation may be expected to be in evidence.

The Mach angle (Θ) for a V will be a function of the angle between the interplanetary field and the velocity as well as the Mach number. Figure 5 shows the geometry of the situation, giving the equation:

(16) $$M_1 = \frac{\sin(\Psi - \Theta)}{\sin \Theta}$$

In the special case $\vec{B} \perp \vec{u}$, this reduces to the form:

(17) $$M_1 = \frac{1}{\tan \Theta}$$

Similarly, for the cone, ellipsoidal wave fronts make the relation

(18) $$M_1 = \frac{1}{\sin \Theta}$$

which is exact for spherical wave fronts, only approximate. If there is a large discrepancy in the values of V_s and

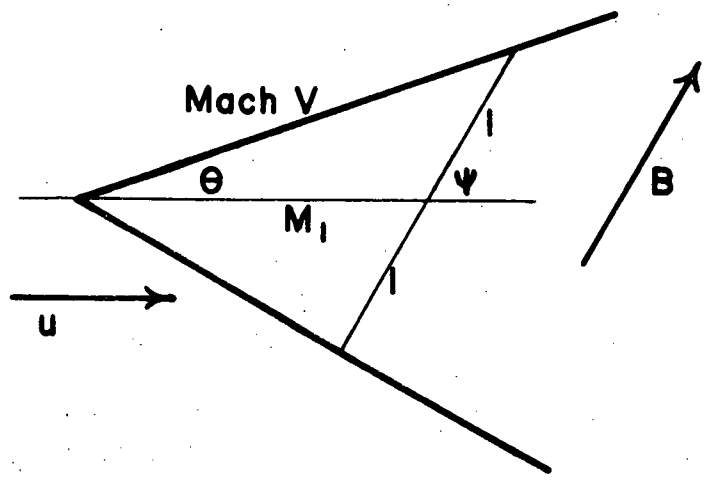

Figure 5. Mach V and wave path.

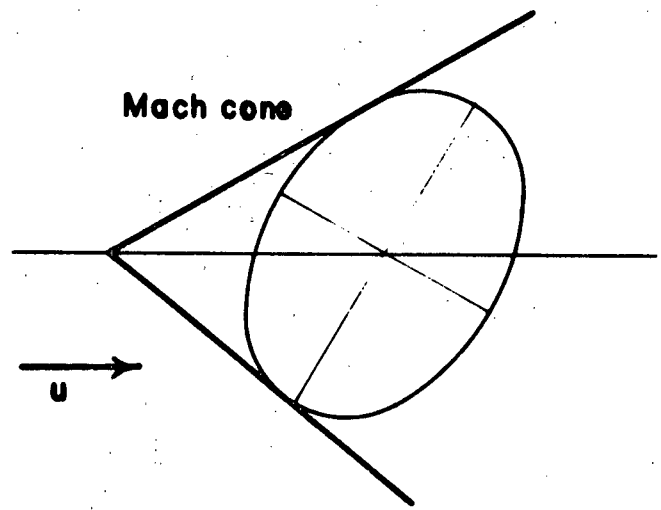

Figure 6. Mach cone and wave front.

V_A , the wave fronts will be approximately spherical and equation (18) can be used.

If $V_s \sim V_A$, coupling occurs between the two magnetosonic modes, indicating that a wave of one type would act as a source for the other. If one is much larger than the other, this effect is negligible. There is also no coupling for propagation parallel to the field, as one of the modes becomes an Alfven wave. Perpendicular to the field, there is only one mode of propagation, and as such a distinct peak of energy must exist. At other angles, the behavior is very complicated, being a regime in which the fast mode is changing from a combined Alfven and perpendicular pressure wave to a combined longitudinal pseudosonic and perpendicular pressure wave. The energy is probably spread over a large region of space, each mode acting as a source for the other. The existence of uncoupled modes parallel and perpendicular to the field should retain the validity of the arguments presented in this thesis despite the coupling, and should accordingly produce magnetic activity peaks at the same positions as for uncoupled propagation.

As $\omega \sim \omega_i$ in the shock front itself, the plasma will be dispersive, particularly for the retarded mode which reaches a resonance point at this frequency

(Denisse and Delcroix 1963). The dispersion will be small for the other modes. The effect will be to break the retarded mode into a dispersed train of waves. In such a train, each frequency would tend to follow its own Mach V or cone.

The geometric attenuation of accelerated mode waves will be similar to that of sound waves, with an energy drop off $\propto \frac{1}{r}$ along the cone. For the guided modes, there should be no geometric attenuation with distance. However in all cases there should still be the equivalent of the rarefaction eating into the shock.

III. INTERPLANETARY SPACE

a. The solar wind

The solar wind is believed to be the expanding solar corona, which Parker (1963) has shown to be unstable — the sun's gravitational field being insufficient to contain the high temperature (10^6°K) gas. It takes about 5 days to pick up speed, and then about four more days to reach the earth's orbit. As the kinetic energy of the gas is much greater than the magnetic field energy, the field lines from the sun are dragged out with the fluid, forming spirals due to the hosepipe effect (Parker 1963). It is, however, a very "gusty" wind, and the field contains many kinks and wiggles. The properties of the wind as measured by satellites (Explorer X, Mariner II, Lunik I and II) in the vicinity of the earth are given in table I.

b. Particle clouds

Another feature of interplanetary space is the particle clouds associated with solar flares. These have higher velocity and density than the solar wind, taking about two days to reach the earth, where they cause magnetic storms. Their properties in the vicinity of the

earth are also summarized in table I. Sudden commencement storms are believed to be caused by such a cloud preceded by a magnetohydrodynamic shock wave.

c. Magnetohydrodynamic theory

Magnetohydrodynamic theory and consequent fluid flow methods requires that:

(i) All disturbance dimensions be much greater than the particle gyration radius.

(ii) All frequencies be less than the ion gyration frequency.

Three cases are considered. These correspond to conditions in the solar wind, the particle cloud, and the region between the shock front and the obstacle. Table II shows the relevant parameters for protons in such regions, using typical values of the variables.

It can be seen that we must deal with dimensions much greater than 100 km. and frequences much less than 1 cps. This does not apply to the shock front itself which contains the mechanism of thermalization of the streaming energy. All the planets fulfill these requirements. The moon is the smallest body considered having a diameter of about 3500 km. The basic period of the disturbance caused by this body will be somewhat larger than $\frac{3500}{u}$ — a factor of 10 greater than the ion cyclotron period.

Table I Properties of the solar wind and particle clouds near the earth.

	Solar Wind	Clouds
streaming velocity	300-500 km/sec.	600-1000 km/sec.
particle density	1-10 /cc.	5-30 /cc.
temperature	$\sim 2 \times 10^5$ °K	$\sim 7 \times 10^5$ °K
contained field	$\sim 5\gamma$	10-50 γ

Table II

Values of relevant parameters in interplanetary space.

Parameter	Wind	Cloud	Shock region
Field strength (γ)	5	20	30
Temperature (°K)	2×10^5	7×10^5	
Thermal velocity $= \sqrt{\frac{\gamma k T}{m_i}}$ km./sec.	70	100	300
$r_i = \frac{m_i V}{q_i B}$ (km.)	140	50	100
$\omega_i = \frac{q_i B}{m_i}$ (cycles/sec.)	.5	2	3
$V_A = \frac{B}{\sqrt{\mu_0 \rho}}$ (km./sec.)	50	100	
$V_s = \sqrt{\frac{2\gamma k T}{m_i}}$ (km./sec.)	100	140	

d. Supersonic flow

It remains to show that the flow is supersonic for all magnetohydrodynamic modes. Two velocities must be considered: the Alfven velocity $V_A = \frac{B}{\sqrt{\mu_0 \rho}}$, and the pseudosonic velocity which is given by Denisse and Delcroix (1963) as:

$$V_s^2 = \frac{n_e m_e V_e^2 + n_i m_i V_i^2}{n_e m_e + n_i m_i}$$

where $m_e V_e^2 = \gamma_e k T_e$ and $m_i V_i^2 = \gamma_i k T_i$

If $n_e = n_i$ and thermal equilibrium exists between ions and electrons, $V_s^2 \simeq \frac{2 \gamma k T}{m_i}$. The value of γ here is not clearly defined, depending on the number of degrees of freedom (s). $\gamma = \frac{s+2}{s}$ For propagation parallel to the field, the magnetoacoustic wave undergoes essentially a one dimensional compression, and as such has $s = 1$, and $\gamma = 3$. Perpendicular to the field, the compression is two dimensional giving $s = 2$, and $\gamma = 2$. The relevant values of V_A and V_S are shown in table II. The streaming velocities are well above the wave velocities, implying supersonic flow with Mach numbers in the range from one to ten.

IV. PREVIOUS SHOCK WORK

a. Kellogg (1962)

Kellogg makes the assumption that the interplanetary field is normal to the streaming velocity, and the plasma can therefore be treated as a hydrodynamic gas using $\gamma = 2$. This is essentially the approximation considered in IIa. His further development uses the results of Hida (1953), in which incompressible flow around the body is assumed after the fluid has passed through a Rankine-Hugoniot shock. The approximations involved make the solution reliable only in a region in front of the sphere, as explained in IIa. In addition Kellogg calculates the flow well behind the sphere along the central streamlines by considering adiabatic expansion of the gas to the pressure of the incoming fluid subsequent to passage through the shock. Combining the Rankine-Hugoniot relations and the expression for adiabatic expansion:

$$(19) \qquad \frac{p_3}{\rho_3^{\gamma}} = \frac{p_2}{\rho_2^{\gamma}} = \frac{p_1}{\rho_3^{\gamma}}$$

he derives the expression:

$$(20) \qquad M_3^2 = \frac{M_1^2 + \frac{2}{\gamma-1}}{\left(\frac{1-\mu^2}{M_1^2}+\mu^2\right)\left[(1+\mu^2)M_1^2 - \mu^2\right]^{\frac{1}{\gamma}}} - \frac{2}{\gamma-1}$$

where $\mu^2 = \frac{\gamma - 1}{\gamma + 1}$

The subscripts indicate the corresponding regions in figure 7.

b. Spreiter and Jones (1963)

Spreiter and Jones use similar approximations to Kellogg. They use the numerical methods of Van Dyke et al (1958, 1959), and allow for compressible hydrodynamic flow behind the shock front. They also allow for the non-sphericity of the magnetosphere using the boundary calculated by Beard (1960) rotated about the sun-earth line. Once again the approximations discussed in IIa are used.

c. Obayashi (1964)

Obayashi discusses the satellite data of 13 space probes interpreting their observations in terms of shock theory. He also discusses their findings of the properties of the interplanetary plasma.

d. Beard (1964)

Beard discusses the phenomenon from a particle viewpoint. He discusses the case of the interplanetary

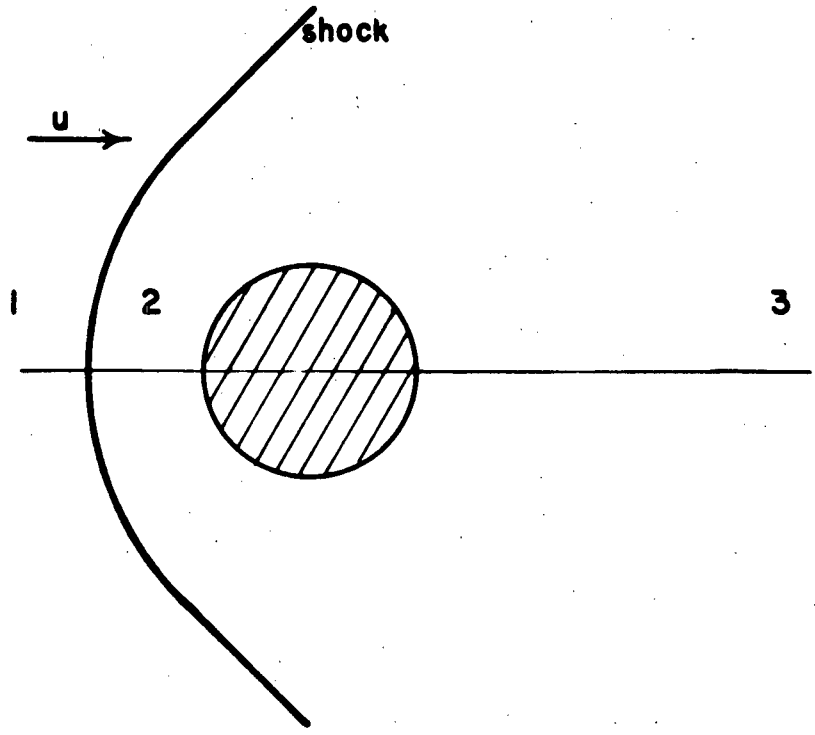

Figure 7. Geometry for Kellogg's equation.

field parallel to the streaming velocity, and concludes that except for a small pocket of particles at the subsolar point, the particles will flow adiabatically around the body. The hosepipe effect (Parker, 1963) implies that the field lines are on the average at 45° to the streamlines (Walters, 1964), and so the configuration $\vec{B_i} \parallel \vec{u}$ is infrequent. For an oblique field, Beard obtains results similar to those of Kellogg.

V. CONDITIONS UNDER WHICH SHOCKS FORM

a. Body with a magnetosphere

The mechanism of formation of a standing shock and bow wave for a body with a magnetosphere has been well described: Kellogg (1962), Spreiter and Jones (1963), Axford (1962), Obayashi (1964), Beard (1964). It involves the interaction of a plasma and a contained magnetic field with a magnetic field. It seems likely that many of the bodies of the solar system have magnetospheres, particularly those with orbits outside Venus. These planets should have a corresponding shock wave.

b. Immersed conducting body

In order to cause little disturbance in the flow, a body would have to allow the passage of lines of force at the velocity of the streaming plasma. Diffusion processes are much too slow. It could be accomplished by a polarization electric field $\vec{E} = \vec{u} \times \vec{B}$. For u = 400 km./sec. and $B = 5\gamma$, $E = 2 \times 10^{-3}$ volts/m. For a body the size of the moon, this represents a voltage of 7000 volts across it. Such a voltage buildup seems unlikely for a body immersed in a highly conducting plasma. It is likely that charge leakage would occur at the sides.

The above process requires the "defreezing" of lines of force at the front of the body, and must result in the formation of a transient atmosphere and ionosphere for such a body. This has been discussed for the moon by Herring and Licht (1959), Singer (1961), Nakada and Mihalov (1962), Weil and Barasch (1963), Gold (1959), and Hinton and Taeusch (1964). Hinton and Taeusch obtain particle densities of 10^6 /cc. for neutral particles, and 10^3 /cc. for ions. The gas pressures are greater than the solar wind pressures, and hence will act as the conducting body which forms the shock. It is likely that the ion sheath, or ionosphere, will be densest on the upstream side of the body.

If a body is surrounded by an atmosphere and ionosphere and no magnetic field, the ionosphere will play the part of the conducting body, and a shock wave can still be expected.

All the bodies of the solar system should fall into one of the above classifications, and may thus be expected to have shock waves unless size considerations exclude them from the regime of hydromagnetic theory.

VI. MAGNETIC ACTIVITY AT LARGE DISTANCES FROM THE SOURCE.

At this stage, the author wishes to suggest the following ideas:

(i) There will be a decrease in magnetic activity within the region behind a shock wave. The activity will be least on the central stream line.

(ii) There will be an increase of magnetic activity in a bow wave. An attempt will be made to justify each of these statements in turn.

a. Activity minimum

As fluid passes through a shock system of the type near the earth, energy is transformed from kinetic streaming energy into thermal energy. A greater flow produces a stronger shock, resulting in a greater loss of streaming energy. This implies that a slow variation in energy flux is attenuated as it passes through the shock. A strict analytic evaluation of this is not possible because of the indeterminate nature of the shock equations. (There is one more variable than equations.) Ideally one would like to evaluate:

$$(21) \qquad \frac{d\left(\rho_3 u_3^2 + p_3\right)}{d\left(\rho_1 u_1^2 + p_1\right)} \simeq \frac{d\left(\rho_3 u_3^2\right)}{d\left(\rho_1 u_1^2\right)}$$

However, it is possible to relate this to the work of Bigg (1963 a, b), as his results are based on the frequency of occurrence of magnetic activity. He uses the numbers of magnetic storms and intervals in which $K_p \geq 30$. As the time intervals on which these are based are long, they are a measure of ΔB rather than of $\frac{dB}{dt}$. If these fluctuations are assumed to be due to pressure changes at the magnetosphere boundary, we are indirectly measuring $\Delta(\rho u^2 + p) \doteq \Delta(\rho u^2)$. (This assumption should be approximately true until ring currents have had time to build up, and even then the magnetic disturbance may give some indication of pressure fluctuations at the boundary.) Thus an attenuation in $\Delta(\rho u^2)$ would imply an attenuation in ΔB. The attenuation in $\Delta(\rho u^2)$ is given by:

$$(22) \qquad \frac{(\rho u^2)_{3\,max} - (\rho u^2)_{3\,min}}{(\rho u^2)_{1\,max} - (\rho u^2)_{1\,min}}$$

$$= \frac{(M_3^2 p_1)_{max} - (M_3^2 p_1)_{min}}{(M_1^2 p_1)_{max} - (M_1^2 p_1)_{min}} \qquad \left(M^2 = \frac{\rho u^2}{\gamma p}\right)$$

where the subscripts apply to the regions shown in figure 7. For large fluctuations, the minimum terms will be much smaller than the maximum terms. For example consider a fluctuation from solar wind to cloud conditions. If the values of table II are used, $\frac{(M_1^2 p_1)_{max}}{(M_1^2 p_1)_{min}} \doteq 16$. Under these circumstances, it becomes possible to ignore the

second terms in equation (22) leading to an attenuation coefficient (A) for large fluctuations in the solar wind:

$$(23) \qquad A = \frac{M_3^2{}_{max}}{M_1^2{}_{max}}$$

A plot of A versus M_1 is shown in figure 8 for $\gamma = 2$ using equation (20). The values used for M_1 and M_3 must be taken at maximum M_1. This should also be the maximum of M_3. Higher M_1 values are usually associated with higher particle fluxes. From figure 8 it can be seen that if this is true, the largest fluctuations would be attenuated the most. However, if the models presented in tables I and II are correct, there is little change in M_1 with activity.

b. Activity maxima

The activity increase in the bow wave can be discussed only qualitatively. The bow wave will exist during quiet conditions, but it is probably of too small an amplitude to produce a measurable effect. During storms the kinetic energy of the streaming fluid increases by one or two orders of magnitude, and there should be an increase in bow wave activity — sufficient perhaps to add noticeable disturbance to an existing storm or active period. It can be shown that under idealized conditions, sufficient energy is available to cause measurable activity.

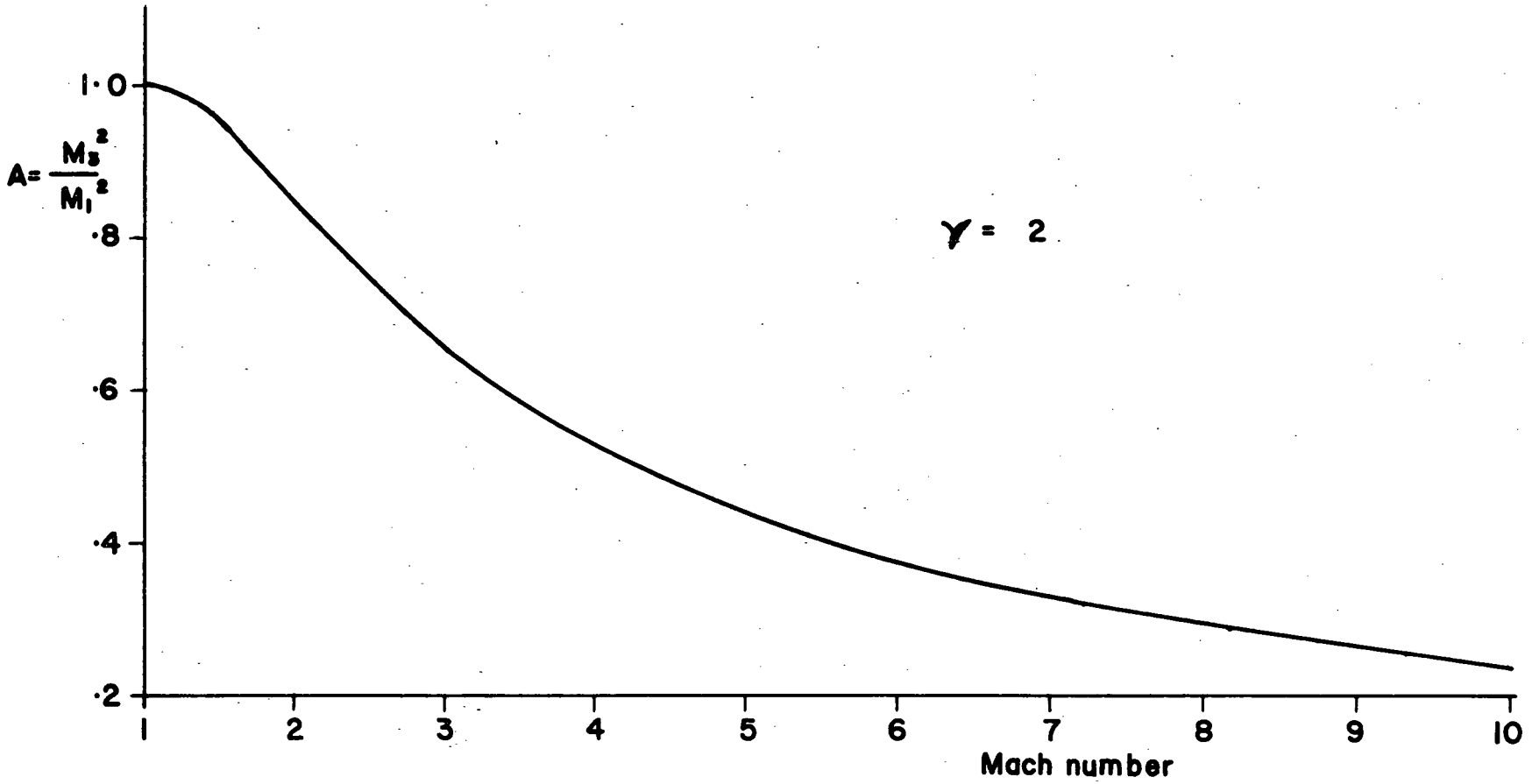

Figure 8. Plot of attenuation coefficient against M_1.

The energy flux incident on the front of a body the size of the magnetosphere (a circle of radius 15 earth radii), during storm conditions (n = 20, u = 1000 km/sec.) is of the order of 10^{22} ergs/sec. If energy of this amount is assumed to spread out in a Mach 3 cone, it is spread over a circle of circumference $2\pi s \tan\theta \doteq 2s$ at a distance s behind the source. For typical interplanetary distance, this is of the order of 10^{8} km. A receiver the size of the magnetosphere would intersect a line segment 10^{5} km. long, and might be expected therefore to receive $\frac{10^{8}}{10^{11}} = 10^{-3}$ of the total energy or 10^{19} ergs/sec. Axford (1963) estimates the energy dissipation during a magnetic storm to be $\sim 10^{18}$ ergs/sec. Even a factor of 10 lower would be capable of producing measurable disturbance. The above calculation of attenuation took into account only geometric effects. If a dropoff $\propto r^{-1.5}$ is used, as in the case of the sonic boom (H. A. Wilson, Jr. 1962), the available energy is reduced by a further factor of 10.

A second independent estimate of the size of the bow wave is developed here. From the second Hugoniot shock equation (11), the following relation

$$(24)\quad p_2 - p_1 = \Delta p = (\rho u_x^2)_1 - (\rho u_x^2)_2 \sim (\rho u_x^2)_1$$

holds across the standing shock in front of the earth, and out to the sides. The assumption is made that the decrease in Δp with distance is the same as for a supersonic aircraft, distances being measured along the cone. From H. A. Wilson, Jr. (1962):

$$\Delta p \propto r^{-\frac{3}{4}} \tag{25}$$

Now if equation (24) is true at point A in figure 14, and equation (25) is assumed to hold from there onwards out along the Mach cone, Δp can be calculated at large distances. For a Mach 3 cone, A is at about 27 earth radii from the earth (figure 14) and about 3 x 27 = 81 earth radii from the vertex of the cone. For a typical interplanetary distance 5×10^7 km., equation (25) implies that $\Delta p = .03\, \Delta p_A$. By comparison with sudden storm commencements, which must also represent a pressure jump $\sim \rho u_x^2$, this represents magnetic fluctuations of a few gammas at a receiver. This is perhaps a little low to produce much difference in magnetic activity, but the uncertainties in the assumptions could easily make a difference of a factor of 10.

For a Mach V, there is no geometric attenuation, and therefore no energy problem. If $V_A > V_S$, the Alfven mode V will be coincident with the fast mode, supplying extra energy in the cone, and extra magnetic activity.

The theory then predicts that there will be an activity minimum behind such a body, and two maxima on each side corresponding to the three modes of propagation. The remainder of this thesis will be concerned with the comparison of experimental evidence with the theory.

VII. EXPERIMENTAL EVIDENCE AND COMPARISON WITH THE THEORY

a. The Planets

It has been suggested by Bigg and De Vaucouleurs (Bigg, 1963 b) that the blue clearings of Mars may be related to magnetic activity frequency. For the purpose of this thesis it will be assumed that the frequency of blue clearings is a maximum when a minimum of magnetic activity exists at Mars and/or in the line of sight between the earth and Mars.

Figures 10 - 13, all from Bigg (1963 a and b), show the dependence of magnetic disturbance frequency on the planetary positions of Mercury, Venus, and the moon, and the blue clearing frequency for Mars. Table III shows the Mach angles that correspond to the peaks indicated by the arrows in figures 10 and 11, and the minima in figure 12. The geometry on which the calculations are based is shown in figure 9. The BB maxima are later associated with a guided slow mode Mach V, and the use of equation (18) rather than (16) to calculate Mach numbers for these peaks must introduce some error. If during storms the interplanetary field is not oriented, on the average, in a direction within about 45° of the streaming velocity, the errors should not be large. It must be pointed out that the angle α in

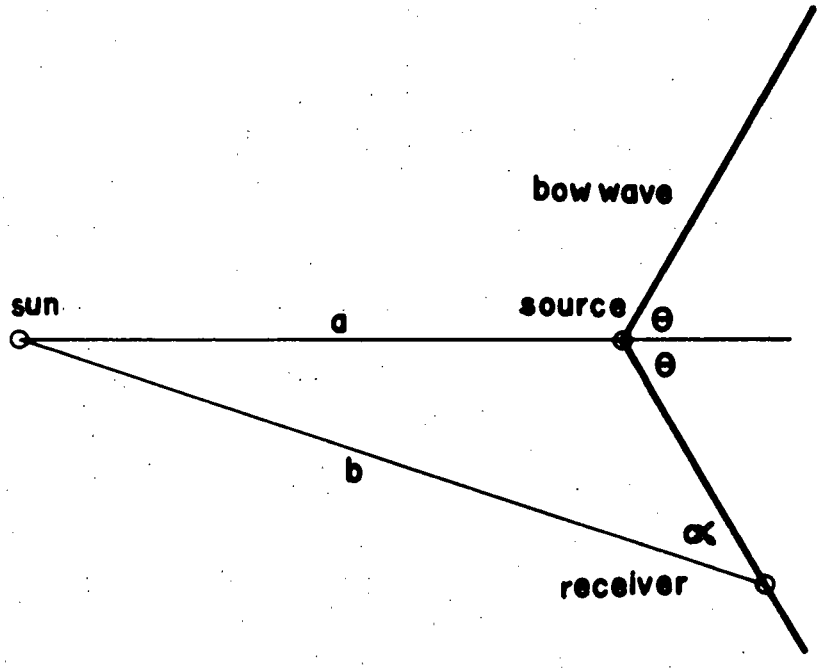

Figure 9. Geometry for table III.

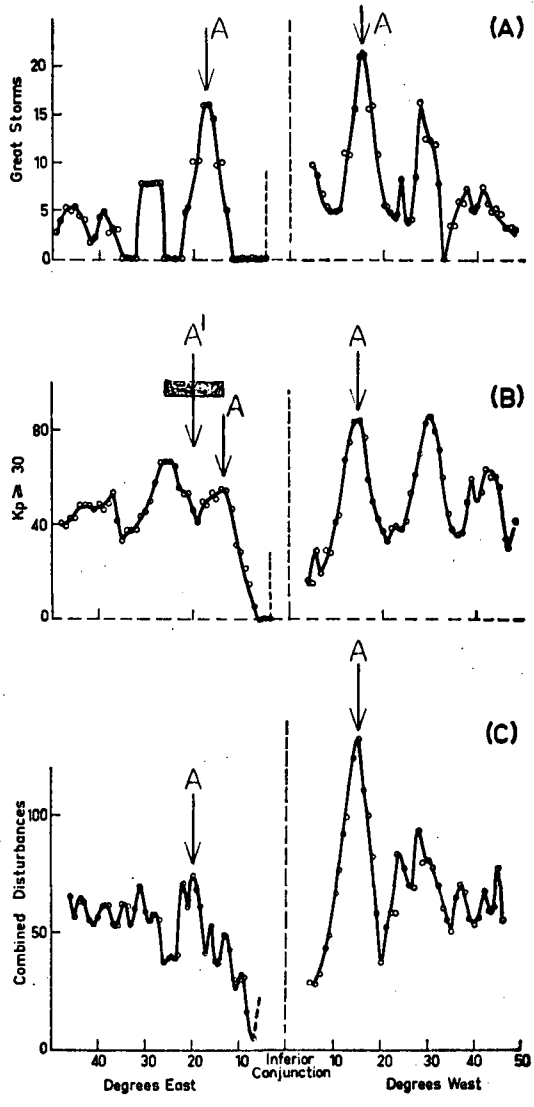

Figure 10. Magnetic activity frequency - Venus. (A) great storms; (B) occasions when $K_p \geq 30$; (C) four sets of data, each set given equal weight.

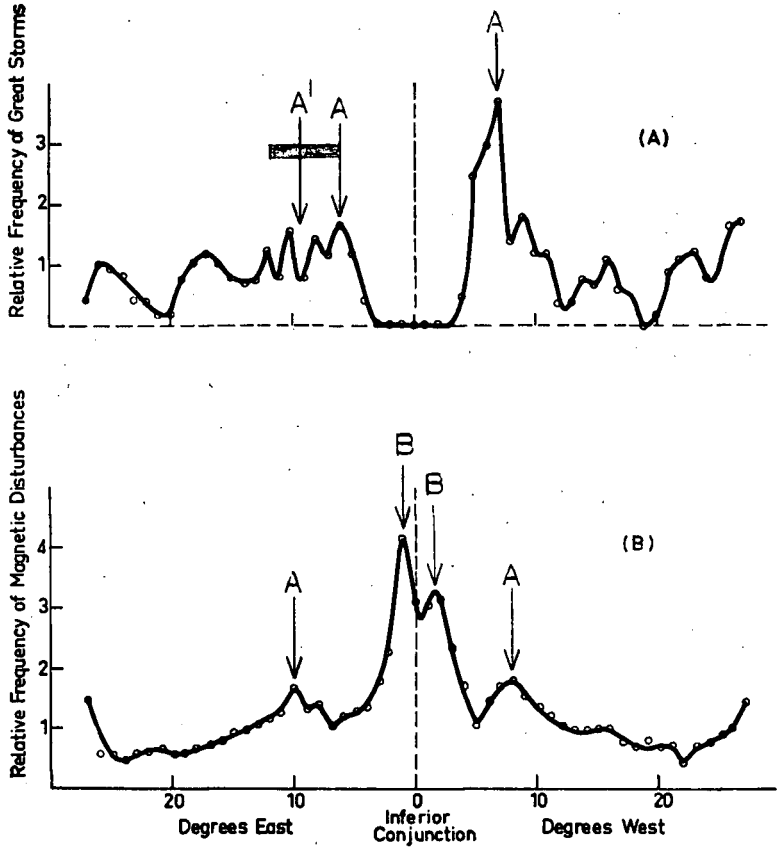

Figure 11. Magnetic activity frequency - Mercury. (A) great storms; (B) four sets of data, each observation given equal weight.

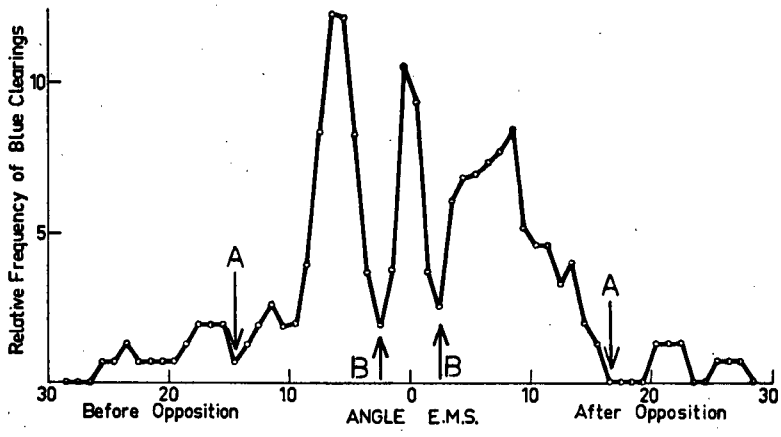

Figure 12. Blue clearing frequency - Mars.

TABLE III. Experimental results in terms of Mach angle and Mach number.

Fig.	Angle 2α between peaks, degrees		$\frac{1}{M_1} = \sin\Theta = \frac{b}{a}\sin\alpha$		$\frac{b}{a}$	Mach angle Θ degrees		Mach number M_1	
	AA	BB	AA	BB		AA	BB	AA	BB
10a	32	?	.382		1.38	22		2.6	
10b	27	?	.324		1.38	19		3.1	
10c	34	?	.405		1.38	24		2.5	
11a	13	none	.292		2.58	17		3.4	
11b	18	2.7	.405	.061	2.58	24	3.5	2.5	16
12	31	5.0	.408	.067	1.52	24	3.8	2.5	15
	AA^1		AA^1			AA^1		AA^1	
10b	34	?	.405		1.38	24		2.5	
11a	16	?	.360		2.58	21		2.8	

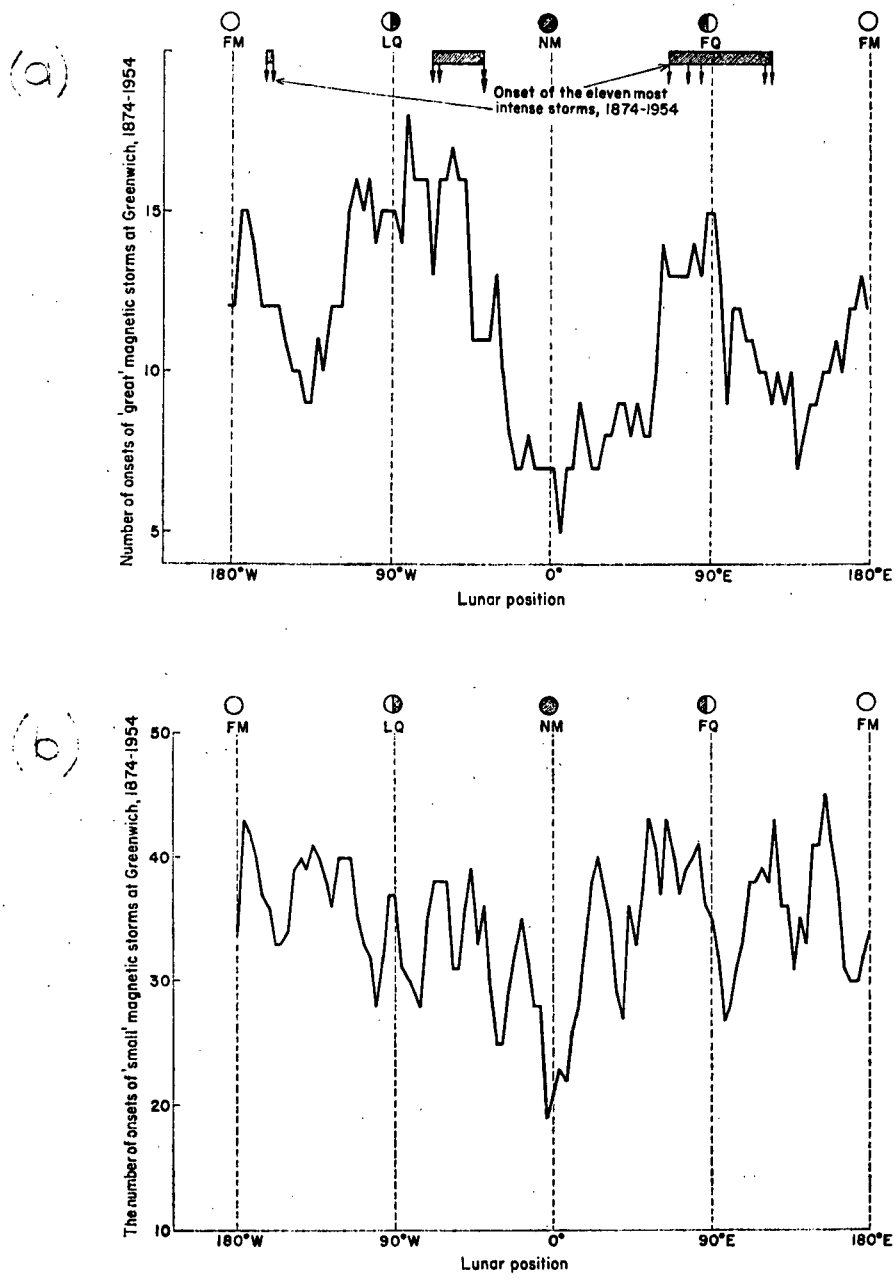

Figure 13. Magnetic activity frequency - Moon.
(a) 112 greatest storms;
(b) small storms.

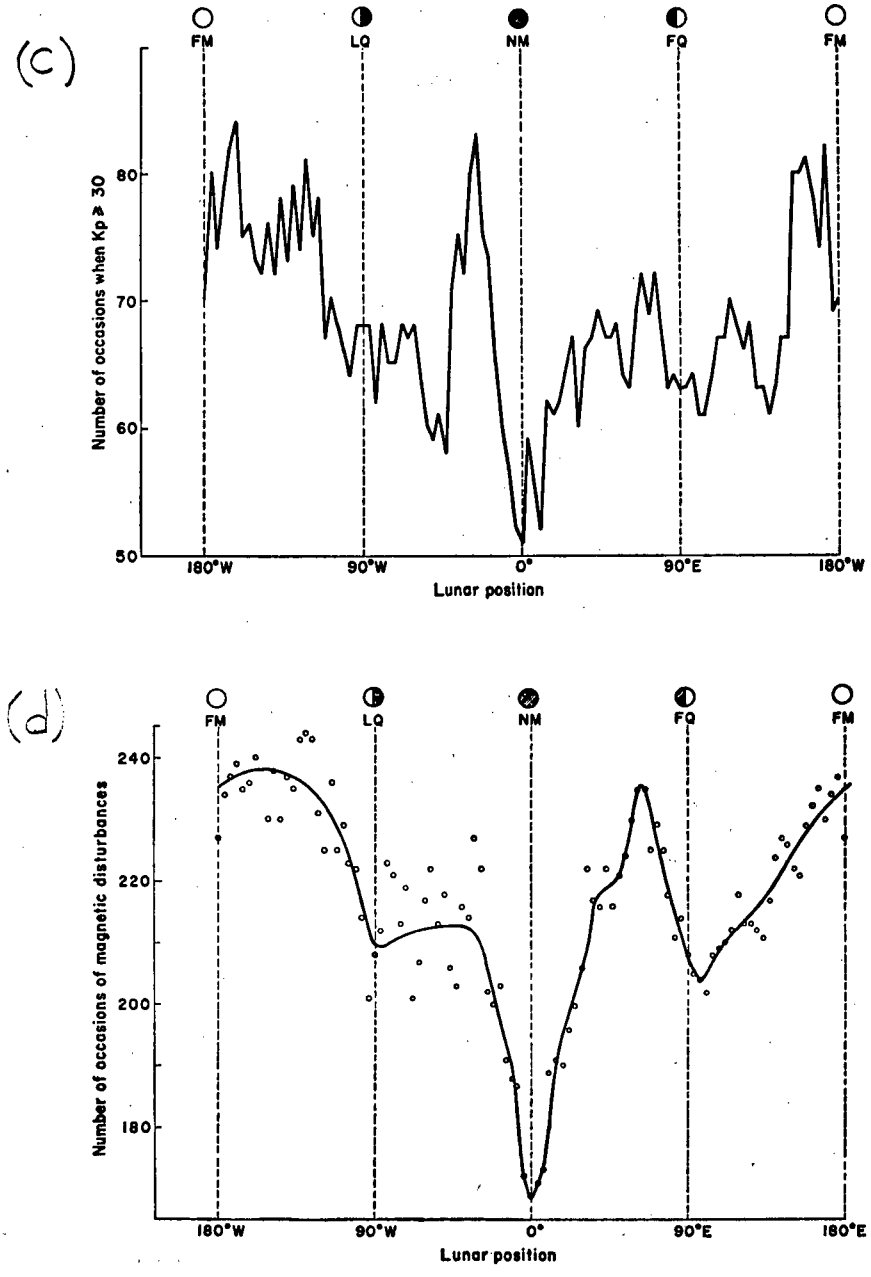

Figure 13. Magnetic activity frequency - Moon.
(c) occasions when $K_p \geq 30$
(d) all disturbances

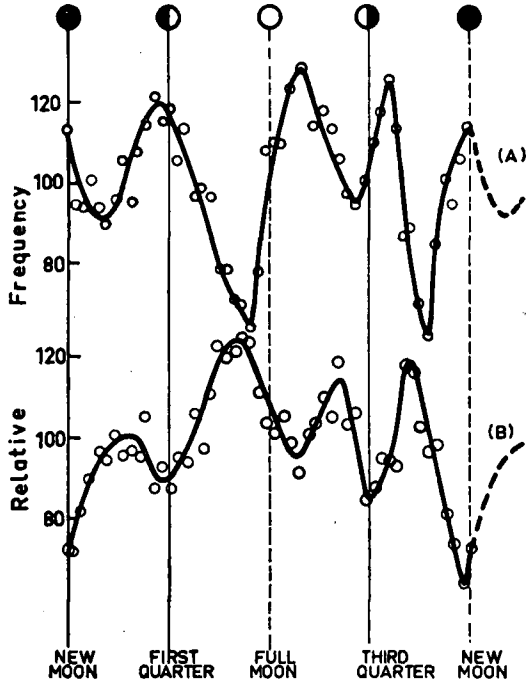

Figure 13. Magnetic activity frequency - Moon.
(e) storms A sudden commencement
B gradual commencement

figures 10 to 12 is the actual angle sun-receiver-source, and not the angle from inferior conjunction. Venus, at inferior conjunction, is at angles from o° to 8° from the sun-earth line, resulting in a scarcity of points in the region 6° east to 6° west. This makes it impossible to determine if BB type maxima appear in figures 10 a, b, c. The few points available and the approaches to the region indicate that there probably are maxima within this region.

In figure 10b, it is not obvious which peak should be used on the east side of the AA maxima. There is not a clearly defined peak rising well above the others. Similarly in figure 11a there are four competing maxima. If instead of taking the inside maxima, the centre A^1 of the region of uncertainty (as shown by the shaded rectangle) is used, the results from these two figures are more consistent with the others. Also the easterly maximum is now at a slightly larger angle than the westerly maximum, as it is for all cases with clearly defined peaks.

The results fit a model with Mach numbers 2.5 and 15 for the two types of bow wave. These we associate with the accelerated and retarded magnetoacoustic modes in turn with the oblique Alfven mode adding to one of these depending on the relative sizes of V_A and V_S .

The lack of BB type maxima in figure 11a is interesting and suggests a number of possible properties of great storms as an explanation:

(i) The interplanetary field may be aligned north-south during a great storm, so that no guided mode waves would reach the receiver.

(ii) The interplanetary field may be broken up (highly turbulent flow) during great storms, restricting propagation by guided modes to short distances.

(iii) The Alfven and sound velocities may be equal implying equipartition between thermal and magnetic energies.

(iv) The field lines may be radial.

At present the author sees no reason to express preference for any one of these possibilities.

The theory predicts that, because of geometrical attenuation, guided modes will have more energy at sufficiently large distances than modes which produce conical bow waves. This is certainly indicated by figure 11b, and it is unfortunate that it is not possible to compare the relative magnitudes of the two types of peaks with those in figure 10c. However, if blue clearing frequency does decrease monotonically with magnetic activity increase, figures 12 and 11b show that the attenuation is in agreement with the theory.

b. The moon

Any effect of the moon on magnetic activity at the earth may be expected to be small as a result of the large size of the magnetosphere (see Figure 14). For instance, at new moon the attenuated region inside the inner bow wave represents a spot of radius 3 earth radii on the front of the magnetosphere, and cannot be expected to have a large effect at the surface of the earth. Any observed variation in magnetic activity frequency with lunar angle must be a function of the angle of incidence of the bow wave on the magnetosphere, the sensitivity of the magnetosphere to pressure fluctuations at the point of incidence, and the efficiency of transfer of energy from this point to the surface of the earth.

Bigg (1963 a, b) obtains the variations shown in figures 13a to e. There is, however, some question as to the statistical significance of these results. If the results are accepted, the maxima in activity for $45° < \alpha < 80°$ indicate that the energy transfer is most effective when the outer bow wave is incident on the side of the magnetosphere. The minimum at new moon could indicate that no energy is received from the outer bow wave at this time. The maximum near full moon can only be associated with the

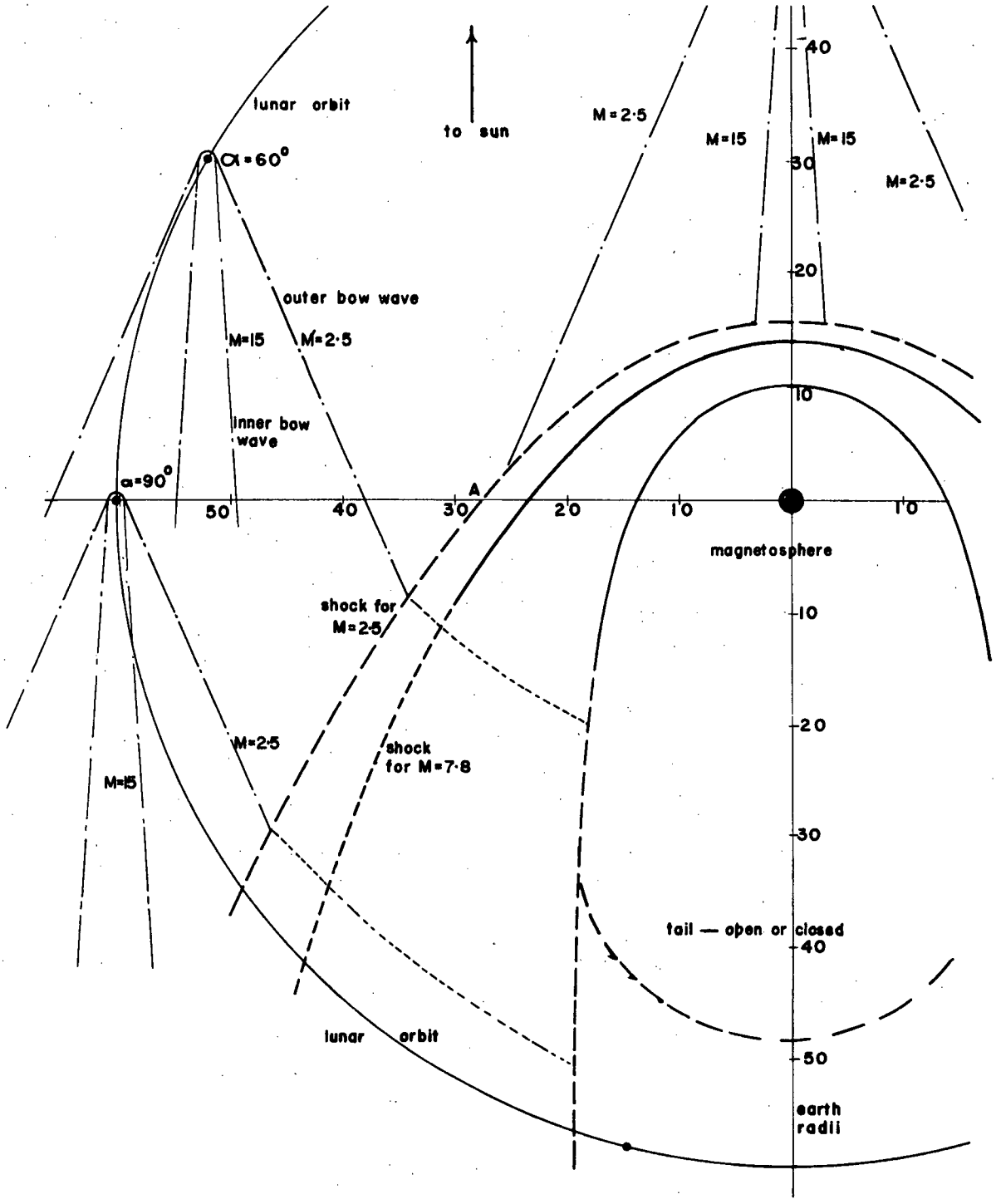

Figure 14. Earth-magnetosphere-moon system, scale drawing.

passage of the moon through one of the following:

(i) The tail of the magnetosphere.

(ii) Field lines shared by the magnetosphere and the interplanetary plasma.

(iii) A subsonic region in the lee of the earth.

With the moon in such regions, the "tail wagging" of the magnetosphere due to variations in the incident magnetized plasma, and any other fluctuations, would be expected to produce a variety of hydromagnetic waves within the magnetosphere which could cause a disturbance increase.

The top line of figure 13e is for sudden commencement storms. This involves the interaction of a hydromagnetic shock wave with the two bow shock waves — a situation very poorly understood. No attempt will be made here to explain the resulting activity frequency plot.

VIII. CONCLUSIONS AND SUMMARY

The interplanetary plasma and magnetic field can be treated as a fluid with supersonic velocity. As such, it forms shock and bow waves at any planet within its flow. The bow wave takes the form of a Mach cone for the accelerated magnetoacoustic mode, and Mach V's for the guided modes (the retarded magnetoacoustic and the Alfven). The Alfven mode coincides with either the cone or the other Mach V, resulting in only two bow waves.

There is an attenuation of magnetic activity frequency behind such an obstacle, the coefficient of energy attenuation being given by equation (23). There is also an increase of magnetic activity along a bow wave. Thus, the experimental results should exhibit a minimum of activity at inferior conjunction, and two maxima on each side. The observed maxima correspond to Mach numbers of 2.5 and 15 implying a velocity ratio between V_A and V_S of 6:1. The theory does not indicate which is greater. There should be geometric energy attenuation $\propto \frac{1}{r}$ along a cone, and none along a V. This is implied by the experimental results. The Mach angle for a V is given by equation (16).

The activity frequency diagrams for the moon are quite different from those for the planets. This is due to the size of the magnetosphere being of the same order as the earth-moon distance. The result is that the magnetosphere intersects large sections of the bow wave pattern, and therefore little magnetic effect should be felt at the surface of the earth. Bigg (1963 a, b) shows an activity dependence on lunar position that can be explained by the presented theory. However, there is doubt that his observations are statistically significant.

Other theories of planetary effects on magnetic activity at the earth are few. Bigg suggests that the planet and the cloud may have electrostatic charges. It is difficult to see how this could produce two maxima on the magnetic activity frequency plot. Indeed, the cloud has to be nearly neutral in order not to fly apart.

Houtgast and van Sluiters (1962) suggested that Venus achieves its effect by having a very large magnetic field. This has been disproved by the results of the Mariner 2 space probe.

There is another possibility that is especially applicable to the case of $\vec{B_i} \perp \vec{v}$. This is that particles are squeezed out along the tubes of force as the

field is compressed. They would move from a field $\simeq 50\gamma$ in the shock to a region where $B \simeq 10\gamma$, conserving $\frac{\frac{1}{2}mv_\perp^2}{B}$ = constant. This constancy of magnetic moment implies that $V_{//}$ (distant) $\simeq$ $V_\perp$ (shock) $\simeq \frac{1}{2} u_1$. It would give the appearance of a Mach V with Mach number 2. This produces only one activity peak, but could combine with one hydromagnetic cone or V to produce the complete pattern. As the velocity of these particles is of the same order as the waves, travelling wave tube amplification of one of the guided modes is possible.

IX. BIBLIOGRAPHY

Axford, W. I., Interaction between solar wind and the earth's magnetosphere. J. Geophys. Res. 67, 3791, 1962.

Axford, W. I., Viscous interaction between the solar wind and the earth's magnetosphere. C.R.S.R. 153, Cornell University Publication, 1963.

Beard, D.B., The interaction of the terrestrial magnetic field with the solar corpuscular radiation. J. Geophys. Res. 65, 3559, 1960.

Beard, D.B., The effect of an interplanetary magnetic field on the solar wind. J. Geophys. Res. 69, 1159, 1964.

Bershader, D., The Magnetodynamics of Conducting Fluids. Stanford University Press, 1959.

Bigg, E. K., The influence of the moon on geomagnetic disturbances. J. Geophys. Res. 68, 1409, 1963 a.

Bigg, E. K., Lunar and planetary influences on geomagnetic disturbances. J. Geophys. Res. 68, 4099, 1963 b.

Courant, R., K. O. Friedrichs, Supersonic Flow and Shock Waves. Interscience Publishers, New York, 1948.

De Hoffman, F., E. Teller, Magnetohydrodynamic shocks. Phys. Rev. 80, 692, 1950.

Denisse, J. F., J. L. Delcroix, Plasma Waves. Interscience Publishers, New York, 1963.

Dugundji, J., J. Aero. Sci. 15, 699, 1948.

Gold, T., in discussion following R. Jastrow, Outer atmospheres of the earth and planets. J. Geophys. Res. 64, 1798, 1959.

Herring, J. R., A. L. Licht, Effect of the solar wind on the lunar atmosphere. Science 130, 266, 1959.

Hida, K. An approximate study on the detached shock wave in front of a circular cylinder and a sphere. J. Phys. Soc. Japan 8, 740, 1953.

Hinton, F. L., D. R. Taeusch, Variation of the lunar atmosphere with the strength of the solar wind. J. Geophys. Res. 69, 1341, 1964.

Houtgast, J., Indication of a magnetic field of the planet Venus. Nature 175, 678, 1955.

Houtgast, J., A. van Sluiters, A new estimate of the strength of the magnetic field of the planet Venus. Nature 196, 462, 1962.

Inouye, Mamanu , Lomas, Comparison of experimental and numerical results - blunt body. NASA TN P, 1426, 1962.

Kellogg, P. J., Flow of plasma around the earth. J. Geophys. Res. 67, 3805, 1962.

Lin, C. C., S. I. Rubinov, J. Math. Phys. 27, 105, 1948.

Montgomery, D., Development of hydromagnetic shocks from large amplitude Alfven waves. Phys. Rev. Letters, 2, 36, 1959.

Nakada, M. P., J. D. Mihalov, Accretion of the solar wind to form a lunar atmosphere. J. Geophys. Res. 67, 1670, 1962.

Neugebauer, M., C. W. Snyder, Preliminary results from Mariner II solar plasma experiment. Science 138, 1095, 1962.

Obayashi, T., Interaction of solar plasma streams with the outer geomagnetic field. J. Geophys. Res. 69, 861, 1964.

Parker, E. N. Interplanetary Dynamical Processes. Interscience Publishers Inc., New York, 1963.

Piddington, J. H., The CIS-Lunar magnetic field. Plan. Space Sci. 9, 305, 1962.

Singer, S. F., Atmosphere near the moon. Astronaut. Acta 7, 135, 1961.

Spreiter, J. R., W. P. Jones, On the effect of a weak interplanetary magnetic field on the interaction between the solar wind and the geomagnetic field. J. Geophys. Res. 68, 3555, 1963.

Van Dyke, D. Milton, The supersonic blunt-body problem - review and extension. J. Aeron. Sci. 25, 485, 1958.

Van Dyke, D. Milton, H. D. Gordon, Supersonic flow past a family of blunt axisymmetric bodies. NASA TR R-1, 1959.

Walters, G. K., Effect of an oblique interplanetary magnetic field on the shape and behaviour of the magnetosphere. J. Geophys. Res. 69, 1769, 1964.

Weil, H., M. L. Barasch, A theoretical lunar ionosphere. Icarus I, 346, 1963.

Wilson, H. A., Jr., Sonic Boom. Sci. Amer., Jan., 36, 1962.

X. APPENDIX - Symbols and Conventions Used.

A attenuation coefficient

B magnetic field

B_o unperturbed magnetic field

B_i interplanetary magnetic field

c_p specific heat at constant pressure

c_v specific heat at constant volume

E electric field

e as subscript denotes "of electron"

i as subscript denotes "of ion" (except B_i)

k Boltzmann's constant

$\vec{k}$ wave propagation vector

m mass of particle

n number density

$P = p_{mag} + p$

p gas pressure

p_{mag} magnetic pressure

q charge

r_i ion gyration radius

r distance

s number of degrees of freedom

T temperature

t as subscript denotes the tangential component

u streaming velocity of a fluid

$u_\perp, u_{//}$ perpendicular and parallel components of u

v particle velocity

V_A Alfven velocity

V_S velocity of sound

v_g group velocity

v_p phase velocity

V volume

x, y, z coordinate axes. As subscript, they denote components

α angle sun - receiver - source

Θ angle between $\vec{k}$ and $\vec{B_o}$

θ Mach angle

ψ angle between $\vec{B_i}$ and $\vec{u}$

γ ratio of specific heats

γ^* defined in the text p. 3

μ_o permeability of free space

ρ density

ω angular frequency

ω_i ion cyclotron frequency